ACS Pharmacology & Translational Science

pubs.acs.org/ptsci

Article

Macrocyclic Gq Protein Inhibitors FR900359 and/or YM-254890—Fit for Translation?

Jonathan G. Schlegel,[⊥] Mariam Tahoun,[⊥] Alexander Seidinger, Jan H. Voss, Markus Kuschak, Stefan Kehraus, Marion Schneider, Michaela Matthey, Bernd K. Fleischmann, Gabriele M. König, Daniela Wenzel, and Christa E. Müller*

Cite This: *ACS Pharmacol. Transl. Sci.* 2021, 4, 888–897

Read Online

ACCESS | Metrics & More | Article Recommendations | Supporting Information

ABSTRACT: Guanine nucleotide-binding proteins (G proteins) transduce extracellular signals received by G protein-coupled receptors (GPCRs) to intracellular signaling cascades. While GPCRs represent the largest class of drug targets, G protein inhibition has only recently been recognized as a novel strategy for treating complex diseases such as asthma, inflammation, and cancer. The structurally similar macrocyclic depsipeptides FR900359 (FR) and YM-254890 (YM) are potent selective inhibitors of the Gq subfamily of G proteins. FR and YM differ in two positions, FR being more lipophilic than YM. Both compounds are utilized as pharmacological tools to block Gq proteins in vitro and in vivo. However, no detailed characterization of FR and YM has been performed, which is a prerequisite for the compounds' translation into clinical application. Here, we performed a thorough study of both compounds' physicochemical, pharmacokinetic, and pharmacological properties. Chemical stability was high across a large range of pH values, with FR being somewhat more stable than YM. Oral bioavailability and brain penetration of both depsipeptides were low. FR showed lower plasma protein binding and was metabolized significantly faster than YM by human and mouse liver microsomes. FR accumulated in lung after chronic intratracheal or intraperitoneal application, while YM was more distributed to other organs. Most strikingly, the previously observed longer residence time of FR resulted in a significantly prolonged pharmacologic effect as compared to YM in a methacholine-induced bronchoconstriction mouse model. These results prove that changes within a molecule which seem marginal compared to its structural complexity can lead to crucial pharmacological differences.

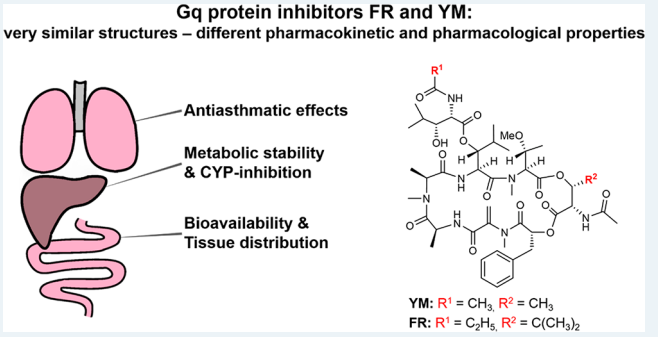

KEYWORDS: *FR900359, Gq inhibitor, metabolic stability, physicochemical properties, pharmacokinetic behavior, YM-254890*

1. INTRODUCTION

The macrocyclic depsipeptide FR900359 (FR, **1**) isolated from the higher plant *Ardisia crenata*,[1] in the leaves of which it is produced by the bacterial endophyte *Candidatus Burkholderia crenata*,[2] acts as a selective Gq protein inhibitor.[3] The structurally closely related natural product YM-254890 (YM, **2**), which had been isolated from a culture broth of *Chromobacterium* sp. QS3666 during the search for novel platelet aggregation inhibitors,[4] was reported to block Gq proteins with similar potency as **1**. These Gq protein inhibitors have become indispensable tool compounds to study Gq protein-mediated signaling induced by G protein-coupled receptors (GPCRs).[5−12] In contrast to the Gi protein inhibitor pertussis toxin and the Gs protein activator choleratoxin, proteins which have been essential tools for studying GPCR signaling for decades, FR and YM are small, macrocyclic, druglike molecules. Several studies provided strong evidence for the potential of Gq protein inhibitors as novel pharmacological agents to treat complex diseases, such as obesity,[13] asthma,[14] and cancer.[17−20] Analogs have been isolated from bacteria[21−23] or prepared by chemical synthesis,[12,24−26] but none of them were significantly more potent than the natural products; in fact, most of them displayed much lower Gq-inhibitory potency or were even inactive.

FR and YM differ only in two residues (see Figure 1), and both inhibitors have been generally regarded as exchangeable due to their almost identical structures. However, in a recent study, we observed that tritiated FR binding to Gq proteins displayed a significantly longer residence time than radiolabeled YM suggesting pseudoirreversible binding of FR but

Received: January 14, 2021
Published: February 19, 2021

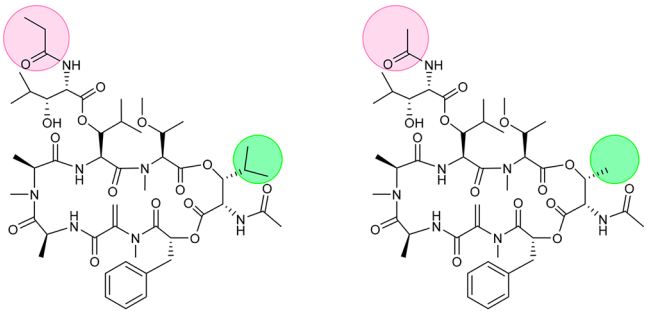

FR900359 (FR, **1**) YM-254890 (YM, **2**)

Figure 1. Chemical structures of the macrocyclic depsipeptidic Gq protein inhibitors FR (**1**) and YM (**2**).

not of YM.[27] Thus, despite their striking structural similarity, these results indicated that both compounds may, in fact, behave differently. However, not much is known about FR's and YM's physicochemical and pharmacokinetic properties, and whether these might result in pharmacodynamic consequences. Such information would be important for guiding biological experiments including preclinical studies and for translation of this class of compounds into the clinics. In the present study, we present essential data providing a basis for future in vivo investigations utilizing FR and YM as tool compounds and promising therapeutic drugs.

2. RESULTS AND DISCUSSION

In a first step, we collected, calculated, and/or determined the physicochemical properties of FR and YM, which are relevant for their application as drug molecules (see Table 1).

Table 1. Physicochemical and Druglike Properties of FR and YM

		FR	YM
exact mass (Da)		1001.53	959.49
heavy atom[a] count		71	68
number of defined stereocenters		11	11
specific rotation[b] ($[\alpha]_D^{20}$)		−54.8	−64.5
rotatable bond count		15	13
polar surface area		285 Å^2	285 Å^2
calculated logP value[c]		1.86	1.37
number of hydrogen bond donors		5	5
number of hydrogen bond acceptors		22	22
solubility in phosphate-buffered saline containing 1% dimethyl sulfoxide (DMSO)[d]		189 ± 17 μM	88 ± 12 μM
plasma protein binding		35%	79%
residence time of tritiated derivative at human platelet membranes[e]	at 37 °C	92.1 min	3.8 min
	at 21 °C	343.3 min	13.4 min

[a]Non-hydrogen atoms [b]Synthetic compounds, measured in methanol, *c* (FR) 0.073 g/mL, *c* (YM) 0.11 g/mL.[24] [c]Calculated logP values were obtained using the StarDrop program. [d]Values represent means ± SD (n = 3). [e]Reference 27.

2.1. Physicochemical and Druglike Properties. Macrocyclic compounds have recently gained much attention in drug development due to their favorable pharmacokinetic properties despite their large molecular weight, which does not conform to Lipinsky's rule of 5.[28] The macrocyclic Gq protein inhibitors FR and YM, which are depsipeptides, differ only in two substituents: FR contains a propionyl instead of an acetyl group and an isopropyl instead of a methyl group (see Figure 1). FR is therefore larger (exact mass: 1001.53 Da) than YM (959.49 Da) and somewhat more lipophilic. Calculated logP values are 1.37 for YM-254890 compared to 1.86 for FR900359 (Table 1). FR and YM are highly complex molecules containing 11 stereocenters and 15 (FR) or 13 (YM) rotatable bonds, respectively. Both compounds were predicted not to be brain-permeable due to their high polar surface area (285 Å^2) and their large number of hydrogen bond donors (5) and acceptors (22). N-Methylation of three of the peptide bonds increases their lipophilicity, which is, however, altogether moderate. The compounds are sufficiently and similarly water-soluble (FR, 189 μM; YM, 88 μM; kinetic solubility). Both display low to moderate plasma protein binding; interestingly, the bound proportion of the more lipophilic FR was significantly lower (35%) compared to that of the more polar analog YM (79%). This property of FR and its relatively high water solubility may be due to the bulky isopropyl substituent, which likely affects the molecule's conformation, crystal packing, and interactions.

One striking difference between FR and YM is their residence time at Gq proteins (Table 1). FR binds pseudoirreversibly to Gq proteins and displays a residence time of 92.1 min at 37 °C compared to 3.8 min for YM.[27] This finding was the first indication that FR and YM are not exchangeable with respect to therapeutic applications despite their high degree of structural similarity.

Thus, FR and YM are macrocyclic molecules with very similar physicochemical properties. The main differences are their lipophilicity, percentage of plasma protein binding, and target residence time.

2.2. Caco-2 Cell Permeation. To experimentally assess the potential of the two Gq protein inhibitors for oral bioavailability, Caco-2 cell permeability assays were performed.[29,30] Caco-2 cells, a human colon adenocarcinoma cell line, are cultured on transwell cell culture plates. After differentiation, they resemble intestinal epithelial cells characterized by the formation of a polarized monolayer with a well-defined brush border on the apical surface expressing various transporters and enzymes as well as intercellular junctions. Results of Caco-2 permeability tests are used to predict intestinal absorption and consequently the bioavailability of a drug when orally administered. Both FR and YM possessed a low apparent permeability coefficient (P_{app}) of 0.4 × 10^{-6} cm/s and 0.1 × 10^{-6} cm/s, respectively (see Table 2). Apical to basolateral transport rates for both compounds were found to be well below the transport rate of the well-penetrating reference drug testosterone and in a similar range as those for the control drugs atenolol and erythromycin, both of which display low peroral absorption. Perhaps due to its higher lipophilicity, Caco-2 cell permeation was somewhat higher for FR as compared to YM. Interestingly, YM showed a P_{app} of 20.9 × 10^{-6} cm/s for basolateral to apical transport resulting in a ratio of 182, indicating very high efflux. This ratio was even higher than that determined for erythromycin included as a reference compound for drugs that are substrates of P-glycoprotein 1 (Pgp, multidrug resistance protein MDR1). In general, a ratio of >2 indicates Pgp transport.[31] The determined ratio shows that YM is indeed a substrate of an efflux transporter such as Pgp. The more lipophilic FR displayed an efflux/influx ratio of 29 indicating that it possesses Pgp substrate properties too, although not as strong as

https://dx.doi.org/10.1021/acsptsci.1c00021
ACS Pharmacol. Transl. Sci. 2021, 4, 888−897

Table 2. Apparent Transport Rates (P_{app}) of YM-254890, FR900359, and Control Compounds in Caco-2 Cells

compound	direction	$P_{app}\cdot10^{-6}$ (cm/s)[a]	ratio (b-a/a-b)[b]	permeability
YM-254890	a-b	0.1 ± 0.0	182	low
	b-a	20.9 ± 2.8		
FR900359	a-b	0.4 ± 0.0	29	low
	b-a	11.5 ± 0.4		
testosterone	a-b	19.2 ± 1.0	2	high
	b-a	39.7 ± 5.2		
erythromycin	a-b	0.1 ± 0.1	106	low
	b-a	11.2 ± 0.4		
atenolol	a-b	0.4 ± 0.0	7	low
	b-a	2.8 ± 0.4		

[a]Apparent permeability (values represent means ± SD, n = 3). [b]High ratio indicates efflux by transporter proteins.

observed for YM. Lacking or low permeation could be advantageous to avoid intoxication upon local, e.g., inhalative treatment. Thus, low absorption combined with high efflux will result in very low oral bioavailability.

2.3. Chemical Stability. Next, we studied the Gq protein inhibitors' chemical stability at different pH values including simulated gastric fluid[32] (pH 1), weakly basic (pH 9), and more strongly basic conditions (pH 11, see Figure 2). The chemical stability of both compounds, FR and YM, was assessed in aqueous solution at 37 °C. A straightforward high-performance liquid chromatography−mass spectrometry (HPLC-MS) method was developed to detect and quantify both compounds and their potential degradation products. In short, HPLC on a reversed-phase column coupled to a single-quadrupole mass spectrometer equipped with an electrospray ionization source was applied for chromatographic separation, and the extract ion chromatograms (EICs) of both compounds were used for identification and quantification (for details see Methods).

We did not observe significant degradation of FR and YM in simulated gastric fluid containing hydrochloric acid (pH 1) and the peptidase pepsin indicating high stability in acid and toward proteolytic cleavage. Both compounds were also stable in an aqueous solution of pH 9. While FR appeared to be completely stable, a slight degradation of YM could be observed (see Figure 2). These results show that both Gq inhibitors would likely survive peroral application. In contrast, at a strongly basic pH value of 11, both compounds were degraded, the more lipophilic FR being significantly more stable than YM. YM decomposed rapidly and completely within 20 min, whereas more than 75% of FR was still present after 4 h of incubation. Interestingly, under all conditions, both depsipeptides formed a small amount of an isomer with equal mass as the parent compound. The isomer could be separated by analytical HPLC from the parent compound, but its structure remains unknown. We propose that the formed isomer constitutes a rearrangement product caused by intramolecular transesterification involving the secondary alcoholic function of the compounds (see Figure 3), a hypothesis that needs to be tested in future studies.

Apart from the mass peaks of the parent compounds and the rearrangement products, a rising number and amount of degradation products were observed with an increased incubation time. Under all conditions, but predominantly at pH 11, hydrated products (FR/YM+H_2O; 1020.19 g/mol; 978.11 g/mol) and the FR/YM "core" structure, lacking the 3-hydroxy-4-methylpentanoate side chain, were detected (816.95 g/mol and 788.9 g/mol, respectively; see Figure 3). The hydrated compounds (FR/YM+H_2O) are likely the result of ester hydrolysis; alternatively, Michael addition reaction to the α,β-unsaturated ketone might occur. These results show that

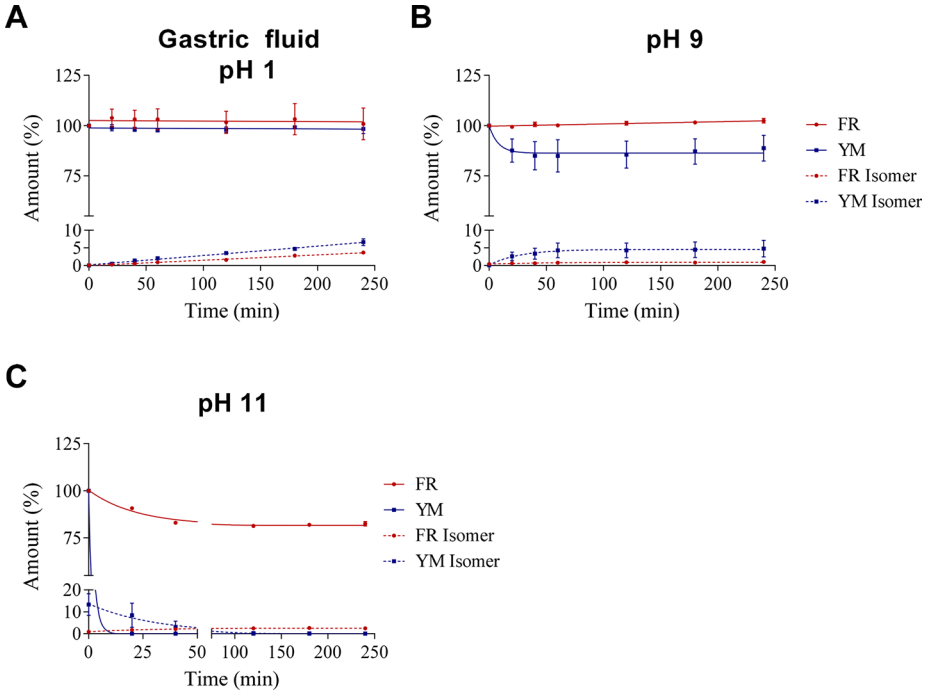

Figure 2. Chemical stability of FR and YM **A**. in simulated gastric fluid, pH 1, **B**. at pH 9, and **C**. at pH 11 (100 μM starting concentration). Solutions were prepared by adding 50 μL of a 1 mM stock solution in DMSO of FR or YM to 450 μL of an aqueous solution A, B, or C. Values represent means ± SEM from three independent experiments. For details, see Methods.

https://dx.doi.org/10.1021/acsptsci.1c00021
ACS Pharmacol. Transl. Sci. 2021, 4, 888−897

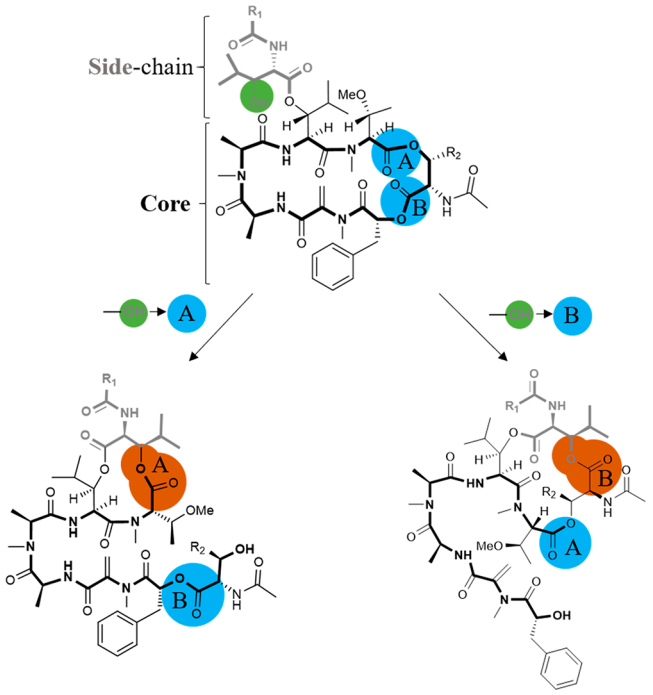

Figure 3. Proposed isomerization reactions (FR: R_1 = CH_2CH_3, R_2 = $CH(CH_3)_2$; YM: R_1 = CH_3, R_2 = CH_3). The secondary alcohol is displayed in green. Esters which possibly take part in the isomerization reaction are highlighted in blue and labeled A or B. Ester bonds newly formed after the reaction are highlighted in dark orange.

the ester functions of YM and FR are reactive toward nucleophiles, and they support the proposed mechanism for the formation of the observed isomers by intramolecular transesterification. Our results indicate that the chemical stability of both FR and YM under physiological conditions is high. Degradation was mainly observed at strongly basic pH values, and the more lipophilic FR was found to be more stable than YM.

2.4. Metabolic Stability. *2.4.1. Stability in Liver Microsomes and Cytochrome P450 Enzyme Inhibition.* Next, we studied the metabolic stability of the compounds in liver microsomal preparations; results are summarized in Table 3.

Table 3. Metabolic Stability of FR and YM in Human and Mouse Liver Microsomes

	$CL_{int,app}$ (μL/min/mg protein)		$t_{1/2}$ (min)	
	human	mouse	human	mouse
FR900359	171.0	237.4	8.1	5.8
YM-254890	50.8	82.2	27.3	16.9
verapamil (control)	134.6	335.7	10.3	4.1

Incubation of FR or YM with human (Figure 4A) and mouse (Figure 4B) liver microsomes resulted in degradation of both compounds, which was more pronounced in mouse as compared to human liver. FR revealed a higher apparent intrinsic clearance ($CL_{int,\ app}$) as compared to YM. Because of its low half-life of only 5.8 min in mouse and 8.1 min in human liver microsomes, FR was completely metabolized within 60 min in both preparations. YM was more stable with $CL_{int,\ app}$ values of 82.2 μL/min/mg protein in mouse and 50.8 μL/min/mg protein in human liver microsomes translating into half-lives of 16.9 min (mouse) and 27.3 min (human). There was approximately one-quarter of YM left after 60 min of incubation in human liver microsomes. The apparent intrinsic clearance of verapamil, which is known to be rapidly metabolized[33] and was therefore included as a positive control, was in a similar range as that of FR. Based on the measured $CL_{int,\ app}$ value, an in vivo CL_{int} can be estimated using suitable scaling factors, i.e., microsomal protein content per gram of liver to be 45 mg of microsomal protein per gram of liver tissue and 26 g (human) or 87 g (mouse) of liver tissue per kilogram of body weight.[34,35] CL_{int} values of FR and YM in humans were determined to be 200.1 mL/min/kg and 59.4 mL/min/kg, respectively. Typically, a CL_{int} (human) below 15 mL/min/kg, between 15−45 mL/min/kg, and above 45 mL/min/kg can be classified as low, intermediate, and high metabolic degradation, respectively.[34,36] Thus, YM and FR were found to be high clearance compounds and do not appear to be suitable for systemic application based on their short half-lives. Due to its somewhat slower metabolic clearance, YM would be preferred for systemic treatment; however, a very short duration of action has to be expected.

Subsequent metabolite identification studies revealed that N/O-dealkylation at various positions of the depsipetides, as well as hydroxylation (observed only for FR), constituted the main metabolic pathways. Structures of specific metabolites have not been identified due to the structural complexity of the compounds which feature many functional groups that may be susceptible to metabolism.

Subsequently, we investigated potential inhibition of cytochrome P450 (CYP enzymes) that is important for drug metabolism by FR and YM. At a concentration of 1 μM, both compounds exhibited only negligible effects on the investigated CYP enzymes. At a very high concentration of 10 μM, inhibition was still negligible to low (Figure S1 of the Supporting Information), except for CYP3A4, which was inhibited by about 50% (FR: 50%, YM: 56%). FR at 10 μM also displayed moderate inhibition of CYP2C8 (30%) and CYP2C19 (38%), whereas inhibition by 10 μM of YM was below 25%. These results indicate that both Gq inhibitors are not expected to interfere with hepatic metabolism of other molecules.

2.4.2. Stability in Lung Tissue and Blood Plasma. FR, which had been found to be less metabolically stable in liver microsomes than YM, was selected for stability testing in lung tissue and blood plasma of mice. The compound was found to be highly stable in both matrices, with more than 90% of the unaltered compound still present after 4 h of incubation in mouse plasma or lung tissue, respectively. A very small amount was converted to its isomer with equal mass (for the presumed structure see Figure 3). This clearly shows that FR is well suited for local, bronchial application.

2.5. In Vivo Bioavailability and Organ Distribution. Next, we studied the concentrations of intact FR and YM in vivo after different application schemes in mice utilizing a recently developed sensitive LC-MS/MS method combined with an optimized extraction procedure.[37]

2.5.1. Intratracheal Application. FR or YM (5 μg) was intratracheally (i.t.) applied to mice on 7 consecutive days. The organs were harvested approximately 45 min after the last FR/YM application, subsequently extracted, and analyzed for FR or YM concentration. High levels of both Gq protein inhibitors were detected in lung and kidney (Figure 5A,B). Only low

https://dx.doi.org/10.1021/acsptsci.1c00021
ACS Pharmacol. Transl. Sci. 2021, 4, 888−897

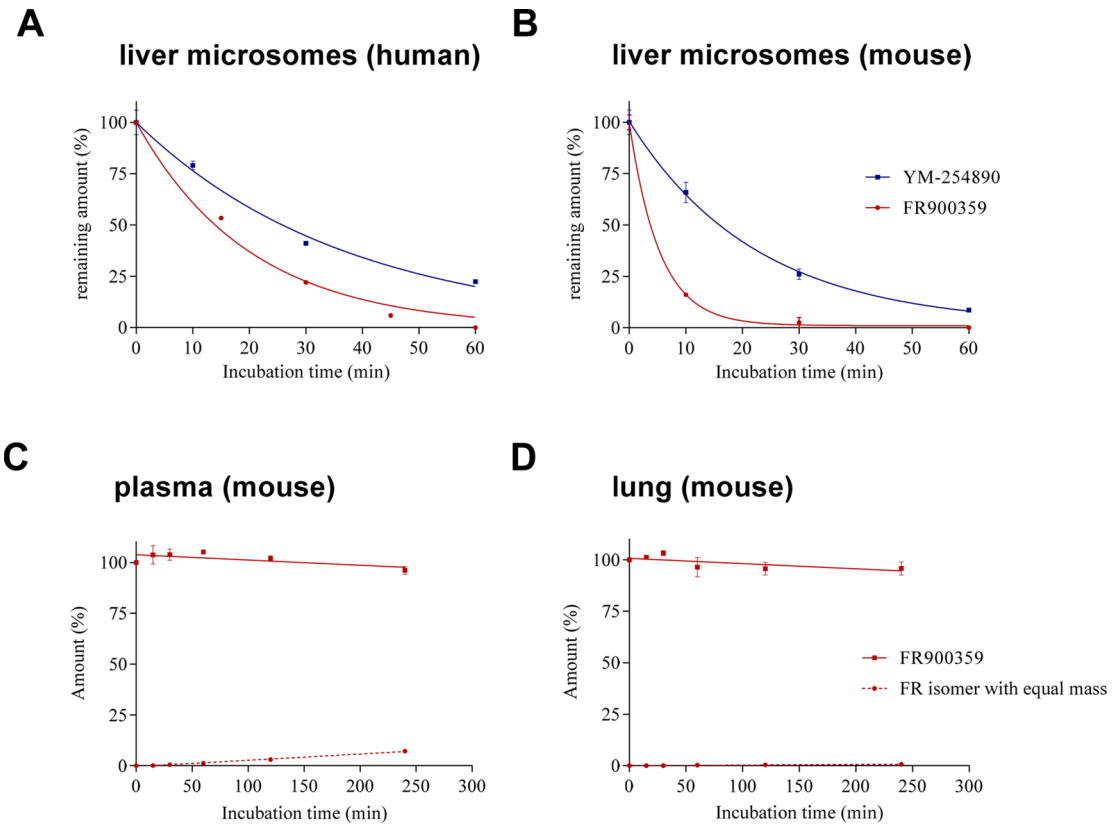

Figure 4. Stability of G protein inhibitors under various conditions: **A**. human liver microsomes (FR, YM); **B**. mouse liver microsomes (FR, YM); **C**. stability in mouse plasma (FR); and **D**. mouse lung tissue (FR). Data represent means ± SEM (n = 3).

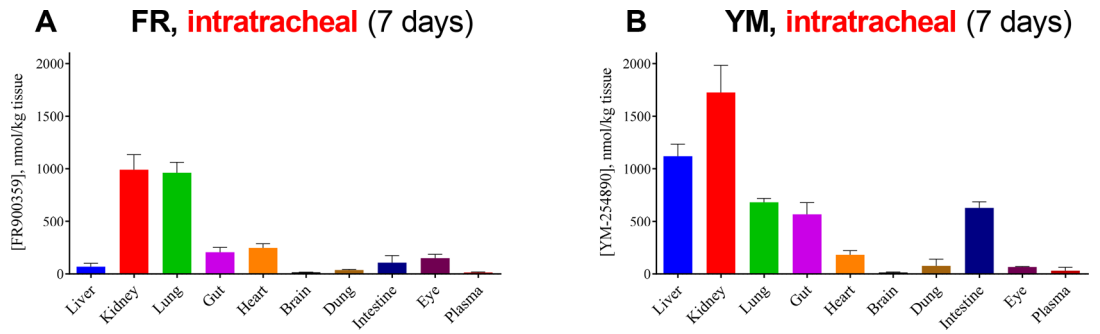

Figure 5. A. Concentration of FR ± SEM and **B**. concentration of YM ± SEM in mouse tissues after intratracheal application of 5 μg of drug on 7 consecutive days. FR and YM levels in organs from three mice were determined.

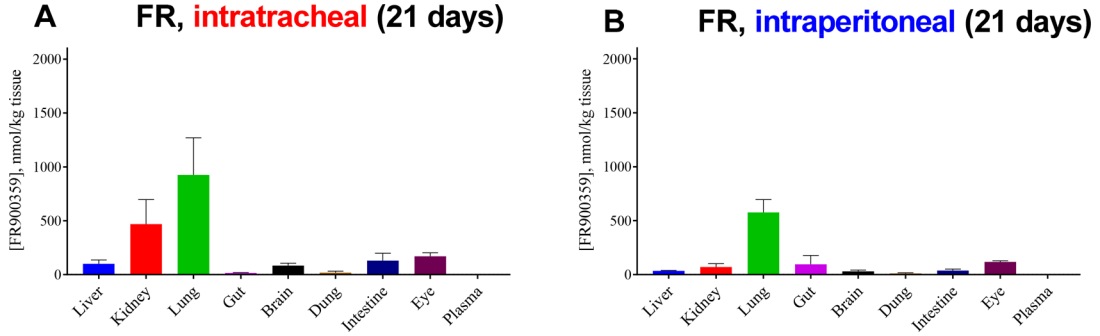

Figure 6. A. Concentration of FR ± SEM in various mouse tissues after intratracheal application of 2.5 μg of FR twice a day for 3 weeks. **B**. Concentration of FR ± SEM in various mouse tissues after intraperitoneal application of 10 μg of FR for 3 weeks (administration from Monday to Friday). FR levels in organs from three mice were determined.

https://dx.doi.org/10.1021/acsptsci.1c00021
ACS Pharmacol. Transl. Sci. 2021, 4, 888−897

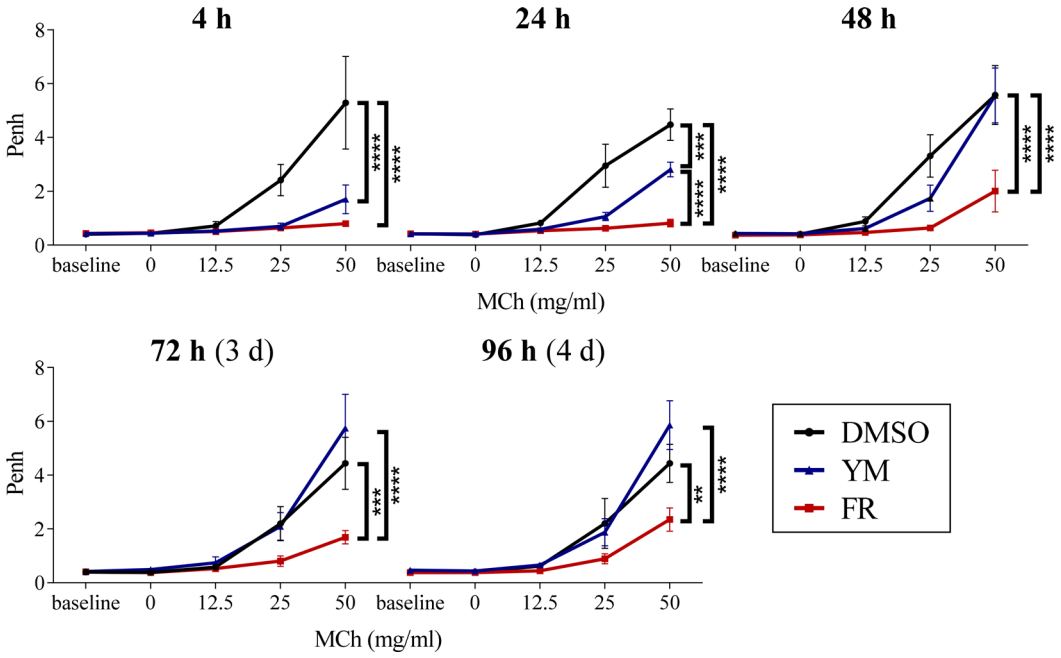

Figure 7. Repeated enhanced pause (Penh) measurements after intratracheal application of FR and YM. Bronchoconstriction was induced by application of methacholine (MCh). FR/YM (2.5 μg) or DMSO was administered intratracheally on day 0. Whole-body plethysmography was carried out after 4 h, 24 h, 48 h, 72 h, and 96 h in the presence of increasing concentrations of MCh which was applied as an aerosol by a nebulizer in the plethysmograph. Data represent means ± SEM (FR, DMSO n = 5; YM n = 4). Statistical significance was assessed by two-way repeated measures ANOVA with Bonferroni's post hoc test. ****, ***, and ** represent a p value < 0.0001, 0.001, and 0.01, respectively.

concentrations of YM and FR were found in brain and blood plasma. Liver, intestine, and lung showed significantly different drug levels of FR as compared to YM. While YM concentrations in liver and kidney were significantly higher than those of FR, the opposite was true for lung, in which higher FR levels than YM levels were detected. These differences are likely due to the different metabolic stabilities of the compounds in liver (compare Figure 4B), FR being less metabolically stable than YM. Moreover, different lipophilicities and different residence times may contribute. FR, which displays a very slow dissociation kinetic,[27] shows higher accumulation in lung as compared to YM likely because it displays pseudoirreversible binding to the Gq proteins and therefore sticks to its targets at the point of entry. Both compounds are preferentially eliminated via the kidneys and, to a smaller but still measurable extent, through feces.

We subsequently studied FR, the preferred Gq inhibitor for intratracheal application, for 21 days. Even after a 3-week treatment, FR levels in lung remained high and were at about the same level as those measured after 1 week (see Figure 6A). These results show that long-term treatment in lung, e.g., for antiasthmatic therapy, is feasible resulting in constantly high drug levels.

2.5.2. Intraperitoneal Application. In further in vivo studies, FR was administered intraperitoneally for 3 weeks. Subsequent extraction and analysis showed that the highest concentrations of FR were again found in the lung (Figure 6B). Direct comparison of i.p. versus i.t. application of FR is shown in Figure 6. In general, FR displayed a similar distribution in the body after both routes of application, but FR levels were overall slightly higher after intratracheal as compared to i.p. application despite slightly lower applied doses. Interestingly, systemic i.p. application resulted in FR levels in the lung comparable to those after local i.t. application. This may be due to high Gq expression in the lung combined with pseudoirreversible binding of FR. FR concentrations determined in the kidneys were significantly higher after intratracheal application, whereas moderate amounts of FR in the gut could only be measured after i.p. application. Independent of the way of application, FR could also be found in the eyes, liver, and intestine. Again, only low to marginal concentrations were found in the brain.

Both in vivo studies showed that FR and YM are not or only marginally able to cross the blood-brain barrier but can be detected in other vital organs, partly in relatively high concentrations in organs which most likely take part in their metabolism or excretion (liver, kidney). Because FR and YM possess low nanomolar IC_{50}/K_i values at their target protein,[22,27] the determined drug concentrations can be expected to be sufficient for pharmacological activity. Besides lung, eye diseases, e.g., uveal melanoma,[16−18] would be the primary targets for local or systemic FR treatment.

2.6. Pharmacological Effects of FR and YM in Mouse Lung Determined by Plethysmography. The results obtained so far in in vitro and in vivo studies indicated that FR and YM may be particularly suited for treating lung disease, since both drugs accumulate in this organ (see Figures 5 and 6). To find out whether the structurally similar Gq inhibitors FR and YM display the same pharmacological properties in vivo, we studied and compared their effect on airways in mice by plethysmography.

Enhanced pause (Penh) displays an index which indicates changes of the airflow waveform in a whole-body plethysmograph that can be correlated with pulmonary reactivity.[38] This noninvasive method enables long-term measurements in vivo in specific individuals and allows assessment of kinetic profiles over a long time course. Previous studies had demonstrated that FR is able to potently induce airway relaxation in mice.[14]

https://dx.doi.org/10.1021/acsptsci.1c00021
ACS Pharmacol. Transl. Sci. 2021, 4, 888−897

Since radiolabeled FR was recently shown to have a much longer residence time than radiolabeled YM[27] (also see Table 1), we wanted to compare the effects of both Gq protein inhibitors on bronchial function. Figure 7 shows the results of repeated Penh measurements with increasing concentrations of methacholine (MCh), a muscarinic acetylcholine receptor agonist inducing bronchoconstriction, after a one-time intratracheal application (i.t.) of FR or YM, respectively. Both Gq protein inhibitors were able to reduce a methacholine-induced Penh increase 4 h after application. However, 48 h after application, mice that had been treated with YM showed a similar reaction as control mice treated with dimethyl sulfoxide (DMSO), in which the Gq protein inhibitors had been dissolved. This indicates, that after 48 h, the antiasthmatic effects of YM were terminated. Interestingly, the effect of FR persisted much longer and could be observed even 96 h after FR application.

These data demonstrate that the significantly longer residence time of the Gq inhibitor FR as compared to YM translates into much longer persistence of the antiasthmatic action.

3. CONCLUSION

Until now, great efforts have been made to evaluate the biochemical and pharmacological profiles of the Gq protein inhibitors FR and YM in order to fully understand their effects on a molecular level.[5,39−41,25,42] The current project focused on a comparison between both compounds and provides first insights into their pharmacokinetic behavior which is a prerequisite for their translational development as therapeutic drugs. Both compounds are Pgp substrates. Interestingly, we found that FR was metabolized significantly faster than YM in human and mouse liver microsomal preparations, which correlated with higher YM levels in vital organs after intratracheal application (Figure 5A,B). Another striking difference was the effect of FR on methacholine-induced bronchoconstriction upon Penh measurements which clearly lasted significantly longer than the effect of YM. This can be explained by the slower dissociation kinetic of FR. These data, along with the determined high FR levels in the lung after local and systemic applications, imply that FR is a prime compound for targeting Gq-based signaling in the respiratory system. However, local administration of the Gq protein inhibitor will be preferred since systemic application can be expected to block Gq signaling throughout the body and is therefore not suitable for use in the clinic. In addition, our results prove that changes within a molecule which seem marginal compared to its structural complexity can lead to crucial pharmacological differences. Additionally, our work demonstrates that differences which were identified by utilizing an artificial and simplified test system like measurement of target residence time of drugs can be transferred to and confirmed in more complex models.

4. METHODS

4.1. Caco-2 Permeability. Caco-2 permeability assays were performed by Pharmacelsus GmbH (Saarbruecken, Germany) in a differentiated Caco-2 cell monolayer-based test system.[15] Transport rates of FR and YM were determined at 10 μM and at a pH of 6.5 (apical, A) and 7.4 (basolateral, B). As reference compounds, testosterone (high transport rates, high bioavailability), atenolol (low transport rates, low bioavailability) and erythromycin (Pgp substrate) were included. Measurements were made at the following time points: 0, 15, 45, and 90 min. Caco-2 cells were differentiated for 21 days in Transwell plates. Bidirectional permeation experiments were performed according to Pharmacelsus in-house protocols. Data represent means ± SEM from three experiments.

4.2. Stability in Simulated Gastric Fluid. Artificial gastric fluid (450 μL, prepared according to the European Pharmacopoeia (Ph. Eur. 10) consisting of 0.32 g of pig pepsin, 0.2 g of NaCl, 8 mL of 1 M HCl, and 100 mL of H_2O) was spiked with 50 μL of FR or YM (1 mM stock solution prepared in DMSO). The mixture was subsequently incubated at 37 °C. Samples (50 μL each) were drawn after 0, 20, 40, 60, 120, 180, and 240 min, treated with ice-cold acetonitrile (1:1), vortexed, and centrifuged for 3 min at 15,000 *g*. An aliquot (50 μL) of the supernatant was transferred to a vial and subjected to LC-MS/MS analysis (see Section Quantitative Analysis of FR and YM by LC-MS/MS for in Vitro Stability Studies). Each experiment was repeated 3 times for each compound.

4.3. Stability in Alkaline Solutions. Alkaline aqueous solutions were prepared by adjusting the pH value of deionized water with NaOH until a pH of 9.0 or 11.0, respectively, was reached. To the alkaline solutions (450 μL) was added 50 μL of FR or YM (1 mM stock solution in DMSO), and the mixtures were incubated at 37 °C. Samples (50 μL each) were drawn after 0, 20, 40, 60, 80, 120, 180, and 240 min. Samples were treated with ice-cold acetonitrile (1:1), vortexed, and centrifuged for 3 min at 15,000 *g*. Aliquots (50 μL) of the supernatant were transferred to a vial and subjected to LC-MS/MS analysis (see Section Quantitative Analysis of FR and YM by LC-MS/MS for in Vitro Stability Studies). Each experiment was repeated 3 times for each compound.

4.4. Quantitative Analysis of FR and YM by LC-MS/MS for in Vitro Stability Studies. Measurements were performed on an Agilent 1260 Infinity HPLC coupled to an Agilent Infinity Lab LC/MSD Single Quadrupole mass spectrometer with an electrospray ion source. Chromatographic separation was performed on an EC 50/3 Nucleodur C18 Gravity, 3 μm (Macherey-Nagel, Dueren, Germany). Mobile phase A consisted of methanol containing 2 mM ammonium acetate and 0.1% formic acid, and mobile phase B consisted of water with 2 mM ammonium acetate and 0.1% formic acid. The run started with 60% A and 40% B for 1 min, followed by a gradient that reached 100% of eluent A after 9 min. Then, the column was flushed for 5 min with 100% of mobile phase A. The flow rate was adjusted to 0.4 mL/min. Positive full scan MS was observed from 200 to 1500 m/z. The peak appeared at 5.7 min for YM-254890 and at 7.4 min for FR900359. For identification and quantification using the Data Analysis program on OpenLab CDS software 2.4, the extracted ion chromatogram (EIC) of 960.5 ± 0.7 m/z was used for YM, and the EIC of 1002.5 ± 0.7 m/z was used for FR. This method was used for the stability studies. Peak areas were evaluated from the EICs and normalized to the FR and YM areas at zero time, and the percentage of remaining compound was calculated. Three independent experiments were performed.

4.5. Metabolic Stability in Human and Mouse Liver Microsomes. Metabolic stability of FR and YM in human and mouse liver microsomes was assessed by Pharmacelsus GmbH (Saarbruecken, Germany). FR or YM (1 μM) was incubated with pooled human or mouse liver microsomes (0.5 mg/mL)

https://dx.doi.org/10.1021/acsptsci.1c00021
ACS Pharmacol. Transl. Sci. 2021, 4, 888−897

in phosphate buffer pH 7.4 in the presence of NADPH and $MgCl_2$. Samples were drawn after 0, 10, 30, and 60 min. The percentage loss of the parent compound was determined by LC-MS analysis. Subsequent metabolite identification in mouse liver microsomes was carried out using HPLC-HRMS by determining accurate masses and fragmentation patterns.

4.6. Metabolic Stability in Mouse Lung Tissue. For stability testing in lung tissue, lungs from four CD1 wild-type mice were pooled, weighed, and subsequently homogenized in a TissueLyzer (Qiagen, Venlo, Netherlands) for 8 min at 50 strokes/min in a precooled tube holder. HEPES buffer, 50 mM, pH 7.4, was added to the homogenate (1 mL of buffer was added to 300 mg of tissue), and the mixture was transferred to a reagent tube. Then, 50 μL of FR solution (1 mM dissolved in DMSO) was added to 450 μL of the lung homogenate and incubated at 37 °C. Samples (6 samples, 80 μL each) were drawn after 0, 15, 30, 60, 120, and 240 min, mixed with ice-cold acetonitrile (1:1), vortexed, and centrifuged for 3 min at 15,000 *g*. An aliquot of 50 μL of the supernatant was transferred to a suitable vial and subjected to LC-MS/MS analysis.

4.7. Stability in Mouse Blood Plasma. Blood plasma of three wild-type CD1 mice was pooled, and 90 μL of the plasma was mixed with 10 μL of FR solution (1 mM in DMSO) and incubated at 37 °C. Samples (6 samples, 10 μL each) were drawn at 0, 15, 30, 60, 120, and 240 min, mixed with ice-cold acetonitrile (1:1), vortexed, and centrifuged for 3 min at 15,000 *g*. Aliquots of 10 μL of the supernatant were transferred to a suitable vial and subjected to LC-MS/MS analysis.

4.8. In Vivo Experiments. Animal experiments were approved by the local ethics committee and carried out in accordance to the guidelines of the German law of protection of animal life with approval by the local government authorities (Landesamt für Natur, Umwelt and Verbraucherschutz Nordrhein-Westfalen, NRW, Germany).

4.8.1. Quantification of FR and YM in Mouse Tissues. In an initial in vivo study, FR or YM (5 μg) was administered intratracheally on 7 consecutive days. In further studies, 10 μg and 2.5 μg of FR, respectively, were administered intraperitoneally (Monday to Friday) and intratracheally (twice a day, Monday to Sunday), respectively, for 3 weeks. In each study, organs from three different mice were harvested and snap-frozen approximately 45 min after the last FR or YM application. FR and YM were extracted by a three-step liquid−liquid extraction method and quantified as previously described by HPLC-ESI-MS/MS.[37] Chromatographic separation was performed using a Dionex Ultimate 3000 (Thermo Fisher Scientific, MA, USA) equipped with an integrated variable wavelength detector coupled to a micrOTOF-Q mass spectrometer (Bruker, MA, USA) with an electrospray ion source. An EC50/2 Nucleodur C18 Gravity 3 μm column (Macherey-Nagel, Dueren, Germany) was used for chromatographic separation. The two mobile phases were A (40% aq. methanol containing 2 mM ammonium acetate and 0.1% formic acid) and B (methanol, 2 mM ammonium acetate, 0.1% formic acid). The run started with 100% A. After 1 min, a gradient was started reaching 100% eluent B within 9 min. Then, the column was flushed for 5 min with solvent B. Positive full scan MS was recorded from 200 to 1500 m/z. The extract ion chromatogram (EIC) of 1002.54 ± 0.01 m/z was used for the identification and quantification of FR by the QuantAnalysis program (Bruker, MA, USA). An EIC of 960.49 ± 0.01 m/z was employed for the identification and quantification of YM.

4.8.2. Whole Body Plethysmography. For i.t. drug application, mice were anaesthetized with isoflurane (5%) and orotracheally intubated using an i.v. cannula (22 G, Vasofix Safely, B. Braun, Melsungen, Germany). The correct positioning of the endotracheal tube was checked under mechanical ventilation with 1.5% isoflurane via a small animal ventilator (MiniVent, Hugo Sachs, Germany). Then, the tube was disconnected from the ventilator, and Gq inhibitors FR or YM (2.5 μg, 1% DMSO in 0.9% NaCl, 50 μL) or the solvent (1% DMSO in 0.9% NaCl, 50 μL) was applied into the tube by a pipet. Thereafter, mechanical ventilation was continued for about 30 s to allow uptake of the liquid. Whole body plethysmography was performed at 4, 24, 48, 72, and 96 h after extubation. Therefore, the awake and unrestrained mice were placed into cylindrical Plexiglas chambers of the whole body plethysmograph (emka Technologies, France). Penh was recorded for 40 s under resting conditions (baseline) and after nebulization of increasing concentrations of methacholine (0, 12.5, 25, and 50 mg/mL).

4.9. Calculation of Compound Properties. LogP, PSA, and peroral and CNS bioavailability were calculated using StarDrop (Optibrium, Cambridge, UK, 2013).

4.10. Data Analysis. *4.10.1. Statistical Analysis.* Statistical significance was determined using a two-way repeated measures ANOVA with a subsequent Bonferroni's post hoc test. Data analysis and plotting were performed using GraphPad PRISM, Version 7.0 (GraphPad, San Diego, CA, USA).

4.10.2. Metabolic Stability. The metabolic degradation process was defined as a first-order decay (eq 1). To obtain a straight line, the natural log of the remaining compound (%) was plotted against time (min). The slope was used to calculate half-lives (eq 2), and $CL_{int,app}$ was determined by using eq 3.[35] Subsequently, eq 4 was applied to obtain $CL_{int,app}$ based on 45 mg of microsomal protein per g of liver tissue and 87 g (mouse) or 26 g (human) of liver tissue per kg body mass.

$$[A]_t = [A]_0 \times e^{-kt} \tag{1}$$

$$t_{1/2} = \frac{\ln(2)}{k} \tag{2}$$

$$CL_{int,app} = \frac{\ln(2)}{t_{1/2}\ [\text{min}]} \times \frac{\text{incubation volume [µL]}}{\text{protein amount [mg]}} \tag{3}$$

$$CL_{int} = CL_{int,app}\ [\mu\text{L/min /mg}] \times \frac{\text{microsomal protein [mg]}}{\text{liver mass [g]}} \times \frac{\text{liver mass [g]}}{\text{body weight [kg]}} \tag{4}$$

■ ASSOCIATED CONTENT

Supporting Information

The Supporting Information is available free of charge at https://pubs.acs.org/doi/10.1021/acsptsci.1c00021.

Inhibition of CYP450 enzymes by FR and YM (PDF)

https://dx.doi.org/10.1021/acsptsci.1c00021
ACS Pharmacol. Transl. Sci. 2021, 4, 888−897

AUTHOR INFORMATION

Corresponding Author

Christa E. Müller − *PharmaCenter Bonn, Pharmaceutical Institute, Pharmaceutical & Medicinal Chemistry, University of Bonn, 53121 Bonn, Germany;* orcid.org/0000-0002-0013-6624; Phone: +49 228 73 2301; Email: christa.mueller@uni-bonn.de

Authors

Jonathan G. Schlegel − *PharmaCenter Bonn, Pharmaceutical Institute, Pharmaceutical & Medicinal Chemistry, University of Bonn, 53121 Bonn, Germany;* orcid.org/0000-0002-6337-0872

Mariam Tahoun − *PharmaCenter Bonn, Pharmaceutical Institute, Pharmaceutical & Medicinal Chemistry, University of Bonn, 53121 Bonn, Germany*

Alexander Seidinger − *Department of Systems Physiology, Medical Faculty, Ruhr University Bochum, 44801 Bochum, Germany*

Jan H. Voss − *PharmaCenter Bonn, Pharmaceutical Institute, Pharmaceutical & Medicinal Chemistry, University of Bonn, 53121 Bonn, Germany*

Markus Kuschak − *PharmaCenter Bonn, Pharmaceutical Institute, Pharmaceutical & Medicinal Chemistry, University of Bonn, 53121 Bonn, Germany*

Stefan Kehraus − *Institute for Pharmaceutical Biology, University of Bonn, 53115 Bonn, Germany*

Marion Schneider − *PharmaCenter Bonn, Pharmaceutical Institute, Pharmaceutical & Medicinal Chemistry, University of Bonn, 53121 Bonn, Germany*

Michaela Matthey − *Department of Systems Physiology, Medical Faculty, Ruhr University Bochum, 44801 Bochum, Germany*

Bernd K. Fleischmann − *Institute of Physiology I, Life & Brain Center, Medical Faculty, University of Bonn, 53105 Bonn, Germany*

Gabriele M. König − *Institute for Pharmaceutical Biology, University of Bonn, 53115 Bonn, Germany;* orcid.org/0000-0003-0003-4916

Daniela Wenzel − *Department of Systems Physiology, Medical Faculty, Ruhr University Bochum, 44801 Bochum, Germany; Institute of Physiology I, Life & Brain Center, Medical Faculty, University of Bonn, 53105 Bonn, Germany*

Complete contact information is available at: https://pubs.acs.org/10.1021/acsptsci.1c00021

Author Contributions

⊥J.G.S. and M.T. contributed equally.

Notes

The authors declare no competing financial interest.

ACKNOWLEDGMENTS

This study was supported by the Deutsche Forschungsgemeinschaft (FOR2372, MU-1665/7-2, WE 4461/2-1 and -2, and FL 276/8-1 and -2).

REFERENCES

(1) Fujioka, M., Koda, S., Morimoto, Y., and Biemann, K. (1988) Structure of FR900359, a cyclic depsipeptide from *Ardisia crenata Sims*. *J. Org. Chem. 53*, 2820−2825.

(2) Carlier, A., Fehr, L., Pinto-Carbó, M., Schäberle, T., Reher, R., Dessein, S., König, G., and Eberl, L. (2016) The genome analysis of *Candidatus* Burkholderia crenata reveals that secondary metabolism may be a key function of the *Ardisia crenata* leaf nodule symbiosis. *Environ. Microbiol. 18*, 2507−2522.

(3) Takasaki, J., Saito, T., Taniguchi, M., Kawasaki, T., Moritani, Y., Hayashi, K., and Kobori, M. (2004) A novel $G\alpha_{q/11}$-selective inhibitor. *J. Biol. Chem. 279*, 47438−47445.

(4) Taniguchi, M., Nagai, K., Arao, N., Kawasaki, T., Saito, T., Moritani, Y., Takasaki, J., Hayashi, K., Fujita, S., Suzuki, K.-i., and Tsukamoto, S.-i. (2003) YM-254890, a novel platelet aggregation inhibitor produced by *Chromobacterium* sp. QS3666. *J. Antibiot. 56*, 358−363.

(5) Schrage, R., Schmitz, A.-L., Gaffal, E., Annala, S., Kehraus, S., Wenzel, D., Büllesbach, K. M., Bald, T., Inoue, A., Shinjo, Y., Galandrin, S., Shridhar, N., Hesse, M., Grundmann, M., Merten, N., Charpentier, T. H., Martz, M., Butcher, A. J., Slodczyk, T., Armando, S., Effern, M., Namkung, Y., Jenkins, L., Horn, V., Stößel, A., Dargatz, H., Tietze, D., Imhof, D., Galés, C., Drewke, C., Müller, C. E., Hölzel, M., Milligan, G., Tobin, A. B., Gomeza, J., Dohlman, H. G., Sondek, J., Harden, T. K., Bouvier, M., Laporte, S. A., Aoki, J., Fleischmann, B. K., Mohr, K., König, G. M., Tüting, T., and Kostenis, E. (2015) The experimental power of FR900359 to study G_q-regulated biological processes. *Nat. Commun. 6*, 10156.

(6) Bolognini, D., Moss, C. E., Nilsson, K., Petersson, A. U., Donnelly, I., Sergeev, E., König, G. M., Kostenis, E., Kurowska-Stolarska, M., Miller, A., Dekker, N., Tobin, A. B., and Milligan, G. (2016) A novel allosteric activator of free fatty acid 2 receptor displays unique G_i-functional bias. *J. Biol. Chem. 291*, 18915−18931.

(7) Carr, R., Koziol-White, C., Zhang, J., Lam, H., An, S. S., Tall, G. G., Panettieri, R. A., and Benovic, J. L. (2016) Interdicting G_q activation in airway disease by receptor-dependent and receptor-independent mechanisms. *Mol. Pharmacol. 89*, 94−104.

(8) Kim, S. H., MacIntyre, D. A., Hanyaloglu, A. C., Blanks, A. M., Thornton, S., Bennett, P. R., and Terzidou, V. (2016) The oxytocin receptor antagonist, Atosiban, activates pro-inflammatory pathways in human amnion via $G_{\alpha i}$ signalling. *Mol. Cell. Endocrinol. 420*, 11−23.

(9) Liao, Y., Lu, B., Ma, Q., Wu, G., Lai, X., Zang, J., Shi, Y., Liu, D., Han, F., and Zhou, N. (2016) Human neuropeptide S receptor is activated via a $G\alpha_q$ protein-biased signaling cascade by a human neuropeptide S analog lacking the C-terminal 10 residues. *J. Biol. Chem. 291*, 7505−7516.

(10) Badolia, R., Inamdar, V., Manne, B. K., Dangelmaier, C., Eble, J. A., and Kunapuli, S. P. (2017) G_q pathway regulates proximal C-type lectin-like receptor-2 (CLEC-2) signaling in platelets. *J. Biol. Chem. 292*, 14516−14531.

(11) Pfeil, E. M., Brands, J., Merten, N., Vögtle, T., Vescovo, M., Rick, U., Albrecht, I.-M., Heycke, N., Kawakami, K., Ono, Y., Ngako Kadji, F. M., Hiratsuka, S., Aoki, J., Häberlein, F., Matthey, M., Garg, J., Hennen, S., Jobin, M.-L., Seier, K., Calebiro, D., Pfeifer, A., Heinemann, A., Wenzel, D., König, G. M., Nieswandt, B., Fleischmann, B. K., Inoue, A., Simon, K., and Kostenis, E. (2020) Heterotrimeric G protein subunit $G\alpha_q$ is a master switch for $G\beta\gamma$-mediated calcium mobilization by Gi-coupled GPCRs. *Mol. Cell 80*, 940.

(12) Zhang, H., Nielsen, A. L., and Strømgaard, K. (2020) Recent achievements in developing selective G_q inhibitors. *Med. Res. Rev. 40*, 135−157.

(13) Klepac, K., Kilić, A., Gnad, T., Brown, L. M., Herrmann, B., Wilderman, A., Balkow, A., Glöde, A., Simon, K., Lidell, M. E., Betz, M. J., Enerbäck, S., Wess, J., Freichel, M., Blüher, M., König, G., Kostenis, E., Insel, P. A., and Pfeifer, A. (2016) The G_q signalling pathway inhibits brown and beige adipose tissue. *Nat. Commun. 7*, 10895.

(14) Matthey, M., Roberts, R., Seidinger, A., Simon, A., Schröder, R., Kuschak, M., Annala, S., König, G. M., Müller, C. E., Hall, I. P., Kostenis, E., Fleischmann, B. K., and Wenzel, D. (2017) Targeted inhibition of G_q signaling induces airway relaxation in mouse models of asthma. *Sci. Transl. Med. 9*, eaag2288.

(15) van Breemen, R. B., and Li, Y. (2005) Caco-2 cell permeability assays to measure drug absorption. *Expert Opin. Drug Metab. Toxicol. 1*, 175−185.

(16) Sun, H., Chow, E. C., Liu, S., Du, Y., and Pang, K. S. (2008) The Caco-2 cell monolayer: usefulness and limitations. *Expert Opin. Drug Metab. Toxicol. 4*, 395−411.
(17) Onken, M. D., Makepeace, C. M., Kaltenbronn, K. M., Kanai, S. M., Todd, T. D., Wang, S., Broekelmann, T. J., Rao, P. K., Cooper, J. A., and Blumer, K. J. (2018) Targeting nucleotide exchange to inhibit constitutively active G protein α subunits in cancer cells. *Sci. Signaling 11*, eaao6852.
(18) Annala, S., Feng, X., Shridhar, N., Eryilmaz, F., Patt, J., Yang, J., Pfeil, E. M., Cervantes-Villagrana, R. D., Inoue, A., Häberlein, F., Slodczyk, T., Reher, R., Kehraus, S., Monteleone, S., Schrage, R., Heycke, N., Rick, U., Engel, S., Pfeifer, A., Kolb, P., König, G., Bünemann, M., Tüting, T., Vázquez-Prado, J., Gutkind, J. S., Gaffal, E., and Kostenis, E. (2019) Direct targeting of $G\alpha_q$ and $G\alpha_{11}$ oncoproteins in cancer cells. *Sci. Signal. 12*, eaau5948.
(19) Lapadula, D., Farias, E., Randolph, C. E., Purwin, T. J., McGrath, D., Charpentier, T. H., Zhang, L., Wu, S., Terai, M., Sato, T., Tall, G. G., Zhou, N., Wedegaertner, P. B., Aplin, A. E., Aguirre-Ghiso, J., and Benovic, J. L. (2019) Effects of oncogenic $G\alpha_q$ and $G\alpha_{11}$ inhibition by FR900359 in uveal melanoma. *Mol. Cancer Res. 17*, 963−973.
(20) Chua, V., Lapadula, D., Randolph, C., Benovic, J. L., Wedegaertner, P. B., and Aplin, A. E. (2017) Dysregulated GPCR signaling and therapeutic options in uveal melanoma. *Mol. Cancer Res. 15*, 501−506.
(21) Taniguchi, M., Suzumura, K.-i., Nagai, K., Kawasaki, T., Takasaki, J., Sekiguchi, M., Moritani, Y., Saito, T., Hayashi, K., Fujita, S., Tsukamoto, S.-i., and Suzuki, K.-i. (2004) YM-254890 analogues, novel cyclic depsipeptides with $G\alpha_{q/11}$ inhibitory activity from *Chromobacterium* sp. QS3666. *Bioorg. Med. Chem. 12*, 3125−3133.
(22) Reher, R., Kuschak, M., Heycke, N., Annala, S., Kehraus, S., Dai, H.-F., Müller, C. E., Kostenis, E., König, G. M., and Crüsemann, M. (2018) Applying molecular networking for the detection of natural sources and analogues of the selective Gq protein inhibitor FR900359. *J. Nat. Prod. 81*, 1628−1635.
(23) Hermes, C., Richarz, R., Wirtz, D. A., Patt, J., Hanke, W., Kehraus, S., Voß, J. H., Küppers, J., Ohbayashi, T., Namasivayam, V., Alenfelder, J., Inoue, A., Mergaert, P., Gütschow, M., Müller, C. E., Kostenis, E., König, G. M., and Crüsemann, M. (2021) Thioesterase-mediated side chain transesterification generates potent Gq signaling inhibitor FR900359. *Nat. Commun. 12*, 144.
(24) Xiong, X.-F., Zhang, H., Underwood, C. R., Harpsøe, K., Gardella, T. J., Wöldike, M. F., Mannstadt, M., Gloriam, D. E., Bräuner-Osborne, H., and Strømgaard, K. (2016) Total synthesis and structure-activity relationship studies of a series of selective G protein inhibitors. *Nat. Chem. 8*, 1035−1041.
(25) Xiong, X.-F., Zhang, H., Boesgaard, M. W., Underwood, C. R., Bräuner-Osborne, H., and Strømgaard, K. (2019) Structure-activity relationship studies of the natural product $G_{q/11}$ protein inhibitor YM-254890. *ChemMedChem 14*, 865−870.
(26) Rensing, D. T., Uppal, S., Blumer, K. J., and Moeller, K. D. (2015) Toward the selective inhibition of G proteins: Total synthesis of a simplified YM-254890 analog. *Org. Lett. 17*, 2270−2273.
(27) Kuschak, M., Namasivayam, V., Rafehi, M., Voss, J. H., Garg, J., Schlegel, J. G., Abdelrahman, A., Kehraus, S., Reher, R., Küppers, J., Sylvester, K., Hinz, S., Matthey, M., Wenzel, D., Fleischmann, B. K., Pfeifer, A., Inoue, A., Gütschow, M., König, G. M., and Müller, C. E. (2020) Cell-permeable high-affinity tracers for G_q proteins provide structural insights, reveal distinct binding kinetics and identify small molecule inhibitors. *Br. J. Pharmacol. 177*, 1898−1916.
(28) Lipinski, C. A., Lombardo, F., Dominy, B. W., and Feeney, P. J. (1997) Experimental and computational approaches to estimate solubility and permeability in drug discovery and development settings. *Adv. Drug Delivery Rev. 23*, 3−25.
(29) Lennernäs, H. (1997) Human jejunal effective permeability and its correlation with preclinical drug absorption models. *J. Pharm. Pharmacol. 49*, 627−638.
(30) Yee, S. (1997) In vitro permeability across Caco-2 cells (colonic) can predict in vivo (small intestinal) absorption in man–fact or myth. *Pharm. Res. 14*, 763−766.
(31) Faassen, F. (2003) Caco-2 permeability, P-glycoprotein transport ratios and brain penetration of heterocyclic drugs. *Int. J. Pharm. 263*, 113−122.
(32) Federal Institute of Drugs and Medical Devices. (2020). *European Pharmacopoeia*, 10th ed., Bonn, Germany.
(33) Hamann, S. R., Blouin, R. A., and McAllister, R. G. (1984) Clinical pharmacokinetics of verapamil. *Clin. Pharmacokinet. 9*, 26−41.
(34) Słoczyńska, K., Gunia-Krzyżak, A., Koczurkiewicz, P., Wójcik-Pszczoła, K., Żelaszczyk, D., Popiół, J., and Pękala, E. (2019) Metabolic stability and its role in the discovery of new chemical entities. *Acta Pharm. 69*, 345−361.
(35) Smith, D. A., Beaumont, K., Maurer, T. S., and Di, L. (2019) Clearance in drug design. *J. Med. Chem. 62*, 2245−2255.
(36) McNaney, C. A., Drexler, D. M., Hnatyshyn, S. Y., Zvyaga, T. A., Knipe, J. O., Belcastro, J. V., and Sanders, M. (2008) An automated liquid chromatography-mass spectrometry process to determine metabolic stability half-life and intrinsic clearance of drug candidates by substrate depletion. *Assay Drug Dev. Technol. 6*, 121−129.
(37) Kuschak, M., Schlegel, J. G., Schneider, M., Kehraus, S., Voss, J. H., Seidinger, A., Matthey, M., Wenzel, D., Fleischmann, B. K., König, G. M., and Müller, C. E. (2020) Sensitive LC-MS/MS method for the quantification of macrocyclic $G\alpha_q$ protein inhibitors in biological samples. *Front. Chem. 8*, 833.
(38) Hamelmann, E., Schwarze, J., Takeda, K., Oshiba, A., Larsen, G. L., Irvin, C. G., and Gelfand, E. W. (1997) Noninvasive measurement of airway responsiveness in allergic mice using barometric plethysmography. *Am. J. Respir. Crit. Care Med. 156*, 766−775.
(39) Inamdar, V., Patel, A., Manne, B. K., Dangelmaier, C., and Kunapuli, S. P. (2015) Characterization of UBO-QIC as a $G\alpha_q$ inhibitor in platelets. *Platelets 26*, 771.
(40) Roszko, K. L., Bi, R., Gorvin, C. M., Bräuner-Osborne, H., Xiong, X.-F., Inoue, A., Thakker, R. V., Strømgaard, K., Gardella, T., and Mannstadt, M. (2017) Knockin mouse with mutant $G\alpha_{11}$ mimics human inherited hypocalcemia and is rescued by pharmacologic inhibitors. *JCI Insight 2*, e91079.
(41) Tietze, D., Kaufmann, D., Tietze, A. A., Voll, A., Reher, R., König, G., and Hausch, F. (2019) Structural and dynamical basis of G protein inhibition by YM-254890 and FR900359: An inhibitor in action. *J. Chem. Inf. Model. 59*, 4361−4373.
(42) Boesgaard, M. W., Harpsøe, K., Malmberg, M., Underwood, C. R., Inoue, A., Mathiesen, J. M., König, G. M., Kostenis, E., Gloriam, D. E., and Bräuner-Osborne, H. (2020) Delineation of molecular determinants for FR900359 inhibition of $G_{q/11}$ unlocks inhibition of $G\alpha_s$. *J. Biol. Chem. 295*, 13850.

https://dx.doi.org/10.1021/acsptsci.1c00021
ACS Pharmacol. Transl. Sci. 2021, 4, 888−897